Joule

CellPress

Report

Figures of Merit for Piezoelectrochemical Energy-Harvesting Systems

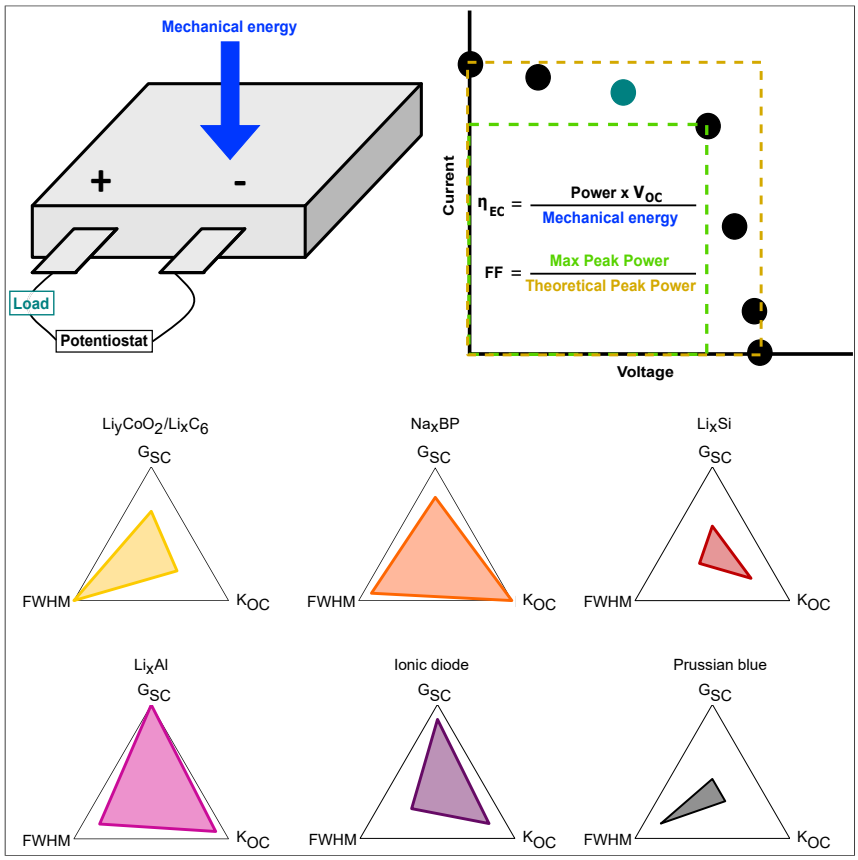

Piezoelectrochemical (PEC) materials use the coupling of mechanical and electrochemical energy to harvest low-frequency mechanical energy, which is possible even in systems such as commercial lithium-ion pouch cells. However, as it is relatively recently discovered in the literature, there has yet to be significant standardization for comparing the efficacy of different PEC harvesters. This article seeks to rectify this problem and proposes several metrics to consistently compare these harvesters, in hopes that using these metrics will enable the design of better-quality harvesters.

Juliane I. Preimesberger, Craig B. Arnold

cbarnold@princeton.edu

HIGHLIGHTS

PEC harvesters exhibit high energy density at low frequency

Optimization of PEC harvesters is challenging without standardized metrics

A unifying framework is proposed to quantify PEC devices for optimal performance

Preimesberger et al., Joule 4, 1893–1906
September 16, 2020
https://doi.org/10.1016/j.joule.2020.07.019

Joule

CellPress

Report

Figures of Merit for Piezoelectrochemical Energy-Harvesting Systems

Juliane I. Preimesberger,[1,3] SeungYeon Kang,[1,2,3] and Craig B. Arnold[1,3,4,*]

SUMMARY

Mechanical micro-energy harvesting is a promising technology that could provide energy to small-scale sensors and other microelectronics without the need for traditional power sources. One such mechanism, called the piezoelectrochemical (PEC) effect, is of particular interest because many PEC systems have higher theoretical energy densities than other mechanical energy harvesters. This energy-harvesting mechanism has been demonstrated in multiple systems, including commonly used electrodes for lithium-ion batteries. However, due to the large variety of materials, it is difficult to consistently compare the utility of PEC systems, which makes the selection and optimization of PEC energy harvesters challenging. Here, we propose using figures of merit including short-circuit current (ΔI_{SC}), open-circuit voltage (ΔV_{OC}), fill factor (*FF*), and efficiency (η_{EC}), which provide a unifying scheme to quantify the performance of different PEC systems. We experimentally validate this approach and demonstrate ways to increase voltage and current outputs of these harvesters.

INTRODUCTION

Mechanical energy harvesting converts mechanical energy into a usable electrochemical micro-energy source that could potentially power microelectronics or sensors.[1–4] However, conventional mechanical energy harvesting materials, including piezoelectrics,[3,4] typically do not perform well at low frequencies of less than 1 Hz and are usually low-energy density. Nonetheless, there are a number of ambient mechanical energy sources that have frequencies of less than 1 Hz,[3,5,6] which cannot be harvested easily by conventional mechanical harvesters. Therefore, there is a desire for high-energy-dense, low-frequency mechanical energy harvesters. A recently identified mechanical micro-energy-harvesting mechanism, called the piezoelectrochemical (PEC) effect, is used in one such harvester.[5–18] PEC systems, also known as mechano-electrochemical systems or strain energy harvesters, among other names, have higher theoretical energy densities and much lower harvesting frequencies than other mechanical energy harvesters.[5] This makes them ideal for harvesting applications that require higher energy densities and lower frequencies than piezoelectrics can provide.

Piezoelectric harvesters require the crystal structure of the material to be changed, creating permanent dipoles that create an electric field.[3,4] Whereas in mechano-electrochemical devices, it is believed that applying stress changes the thermodynamic equilibrium state of the material, which drives ion flux to return the system to equilibrium.[5,10] Therefore, the chemical potential of the mobile ions in a PEC

Context & Scale

Increasing demand for low-energy sources for microelectronics requires energy harvesters that can squeeze energy from ambient sources in the environment. Mechanical energy harvesting has long been a promising ambient energy source, but most conventional mechanical energy harvesters are low in energy density and do not operate effectively below 1 Hz. However, mechanical energy harvesters called piezoelectrochemical or mechano-electrochemical harvesters provide high theoretical energy density and the potential to tap low-frequency mechanical vibrations that cannot be utilized by other mechanical harvesters. Such devices are not commercially viable at this time, but by developing metrics to characterize the efficacy of new piezoelectrochemical harvesters, one can create a framework for selection and optimization leading to improved piezoelectrochemical systems.

material is coupled to mechanical stress, allowing direct conversion of mechanical energy to electrochemical potential. An example of a PEC material is graphite with intercalated mobile ions: as stress is applied, the potential of the intercalated ions changes, making it favorable for ions to move to reach equilibrium. The high theoretical energy density and slow harvesting frequencies of PEC materials are due to the energy-dense faradic reactions and relatively slow kinetic transport of these mobile ions.[5] PEC materials are characterized by a significant volume change during an electrochemical reaction.

As such, it is technically possible that any material that undergoes a volume change during an electrochemical process would be a PEC material. However, in practice, only a few materials that harvest energy in this fashion have been evaluated in recent literature.[5–18] Experimental demonstrations of this effect have been reported in lithium-cobalt-oxide-graphite,[5,7,8] sodium-phosphorus,[6] lithium-carbon,[9] lithium-silicon,[10,11] and lithium-aluminum systems,[12] among others. Our group has previously demonstrated that commercially available lithium-ion pouch cells exhibit this effect and can be used in an energy-harvesting cycle by mechanically loading and unloading the cells.[5,7,8,15] The voltage and current outputs of these harvesters are not high enough for most practical energy-harvesting applications. Significant work needs to be done to design a practical harvester that can be commercially viable. The materials that have been tested so far are likely only a small subset of materials that exhibit this effect and might not be the most effective PEC harvesters possible. For a more systematic search for better PEC harvesters with higher current and voltage outputs, better guidelines are required on how to compare new and existing PEC harvesters.

Still, there is currently no standardized way to compare the energy-harvesting effectiveness of different PEC systems. To address this, we propose figures of merit to compare the performance of different mechano-electrochemical energy harvesters. We derive these figures of merit for PEC systems from the results from our system of commercially available pouch cells, where both the lithium cobalt oxide (LCO) and graphite are PEC materials. Then using these metrics, we compare existing literature values and show that PEC systems, without substantial optimization, are already competitive with piezoelectric systems in terms of normalized energy density. We propose additional parameters analogous to photovoltaic metrics that characterize these systems under practical operating conditions. Finally, we experimentally demonstrate how we can improve the voltage and current output of our pouch cell harvesters by connecting multiple cells together in series or parallel.

RESULTS AND DISCUSSION

Deriving Figures of Merit for PEC Systems

To compare mechanical energy harvesters, we begin with figures of merit such as open-circuit voltage (V_{OC}) and short-circuit current (I_{SC}), which are typically used to characterize energy harvesters like photovoltaic systems and are commonly reported for piezoelectric and PEC systems. Open-circuit voltage is the highest voltage the cell can achieve, and short-circuit current is the current output of the cell at zero voltage, and these values are used in photovoltaics to directly compare systems. For mechano-electrochemical harvesters, we need to define the voltage and current outputs of the PEC effect as the change in potential and current as opposed to the nominal outputs. This way, we can isolate the open-circuit voltage and short-circuit current responses due to added stress from the electrochemical reactions inherent

[1]Department of Mechanical and Aerospace Engineering, Princeton University, Princeton, NJ 08540, USA

[2]Department of Mechanical Engineering, University of Connecticut, Storrs, CT 06269, USA

[3]Princeton Institute for the Science and Technology of Materials (PRISM), Princeton University, Princeton, NJ 08540, USA

[4]Lead Contact

*Correspondence: cbarnold@princeton.edu

https://doi.org/10.1016/j.joule.2020.07.019

to the harvester. However, unlike photovoltaic systems, there are no standardized experimental testing conditions to characterize the performance of a mechanical harvester. Therefore, to reliably compare open-circuit voltage and short-circuit current outputs, we need to account for the input mechanical work.

Previous research has suggested a coupling factor K, which linearly relates the system's change in potential ΔU_0 with applied stress $\Delta\sigma$.[5,7] Previously, this coupling factor was defined as an effective change in voltage with respect to stress, but this factor was dependent on many variables[5,7,15]:

$$K_{eff}(\mathrm{SOC}, \mathrm{SOH}, R, \phi, f) = \frac{\Delta U_0}{\Delta\sigma} \quad \text{(Equation 1)}$$

With this effective coupling factor, state of charge (SOC) and state of health (SOH) of the cell, frequency f, and external resistances R used to measure signal will all affect the coupling factor, in addition to material parameters ϕ. We would like to isolate the effect of material parameters ϕ to determine which PEC material system is better. To do this we fix SOC and SOH of the system, and modify the open-circuit voltage figure of merit and define the open-circuit coupling factor, K_{OC}, as the change in open-circuit voltage with respect to stress:

$$K_{OC}(\phi) = \frac{\Delta V_{OC}}{\Delta\sigma} \quad \text{(Equation 2)}$$

Note that this is still a function of SOC and SOH, but in this paper, we assume that researchers have chosen the optimal SOC and SOH when they present their harvesters, as some papers mention the SOC of their device.[11,12] This coupling factor is not a function of frequency because there is no ion mobility at open-circuit voltage, so ion kinetics are not at play. This figure of merit quantifies the maximum voltage output per unit of the stress of a PEC system and could be used to determine whether the system can provide enough voltage for a specific application.

It has also been shown that current outputs of mechano-electrochemical harvesters are proportional to the applied stress,[6,11] so to compare between different experimental setups, a similar current density coupling factor is needed. We propose a short-circuit current coupling factor G_{SC}, which correlates the change in short-circuit current density ΔJ_{SC} ($\Delta I_{SC}/A$) with applied stress $\Delta\sigma$, where A is the active area of the harvester:

$$G_{SC}(f, \phi) = \frac{\Delta J_{SC}}{\Delta\sigma} \quad \text{(Equation 3)}$$

As stress is applied, the current peaks and then decays to zero as the system equilibrates.[19] Short-circuit current density ΔJ_{SC} is defined from the peak current value ΔI_{SC} (see Figure 1). Note that this is still a function of frequency due to ion kinetics, but here, we make a simplifying assumption that harvesting frequency is sufficiently slow enough for the short-circuit current to fully decay to zero. In our system, we have made sure that the frequency is low enough for the short-circuit current to decay to zero, but other systems[6,12,17] operated at too fast a frequency for this to be true. However, the dependence of ΔI_{SC} on frequency is still unknown, so we do not yet have the tools to account for frequency; hence this assumption is needed.

While short-circuit current and open-circuit voltage outputs are important for the operation of a device, we usually want to compare power and energy densities for micro-energy sources to determine their usefulness as a harvester. Mechano-electrochemical systems[6,11–13,17] sometimes define a theoretical power output as the product of the short-circuit current and open-circuit voltage. Even though the actual

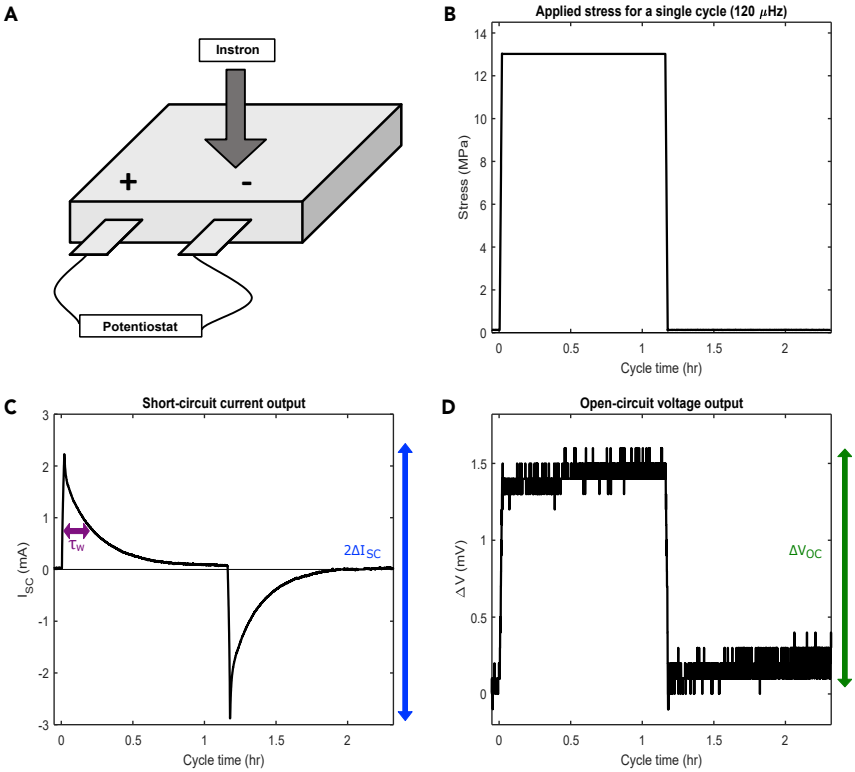

Figure 1. Current and Voltage Measurement Method for PEC Harvesters

(A) Schematic of a commercial pouch cell, connected to a potentiostat and compressed by an Instron.

(B) Profile of the Instron-applied stress for a single cycle at 120 μHz.

(C) The current output of a single harvesting cycle (positive current corresponding to being under stress). FWHM (τ_w) and peak current ΔI_{SC} are labeled.

(D) Open-circuit voltage output of a single cycle. The voltage difference ΔV is with reference to initial open-circuit voltage. The change in open-circuit voltage with stress, ΔV_{OC}, is also labeled.

power density of the device must be lower than this product due to loss and inefficiency, this theoretical power output is a good first approximation for comparing the performance of different devices. Following this logic, we can calculate a normalized theoretical peak power density Λ_{th} using the two coupling factors, calculated as:

$$\Lambda_{th} = \frac{\Delta J_{SC} \Delta V_{OC}}{\Delta \sigma^2} = G_{SC} K_{OC} \qquad \text{(Equation 4)}$$

This normalized peak power density signifies how quickly the system can charge or discharge per unit of stress squared. Like all energy storage devices, there is a trade-off between power and energy density; it is expected that PEC systems would have poor power density but good energy density due to their low operating frequencies.

To estimate normalized energy density per half-cycle, we use the normalized theoretical peak power density Λ_{th} multiplied by an estimated decay time. This decay time is a measure of how quickly the current decays to zero as the cell equilibrates and is related to the differential voltage of the system.[8,19] In principle, we could use the decay rate to calculate energy density; most papers only report a full-

width-half-max (FWHM) of the short-circuit current, which we will call τ_w, and use this to estimate energy density:

$$E_h = \frac{\Delta J_{SC} \Delta V_{OC} \tau_w}{\Delta \sigma^2} = G_{SC} K_{OC} \tau_w \quad \text{(Equation 5)}$$

This is not the theoretical maximum energy per half-cycle, because using τ_w as a decay time will not equal the area under the current-time curve, but it works as an approximation. This figure of merit will tell us the amount of charge the system can store, normalized by stress squared. A higher normalized energy density corresponds to a system that will provide power to a system for a longer period of time, meaning the system can harvest very low-frequency vibrations. If a system can operate at low stresses, this normalized energy density will be larger. This could be useful for many low-stress applications.

To measure these figures of merit for our system, we used an Instron compressive testing machine to uniaxially compress commercially available LCO and graphite pouch cells, as depicted in Figure 1A. The cells were cyclically compressed from 0 to 13 MPa at a frequency of 120 μHz (about 2.3 hours per cycle), and the corresponding short-circuit current or open-circuit voltage response of the cells was measured using a potentiostat. A single cycle of the applied stress profile is plotted in Figure 1B. A characteristic single cycle output of the short-circuit current is plotted in Figure 1C. We have defined the sign convention of the current such that an increase in compressive stress corresponds to an increase of current. Because the current response to stress and the release of stress is symmetric, the peak current (ΔI_{SC}) was taken as half the peak-to-peak current, even though most literature reports the full peak-to-peak values. We found there is a slight asymmetry between the positive and negative peaks, likely due to instrumentation internal resistances, which is why we take the entire peak-to-peak range and divide by two (see Figure S2). Additionally, as depicted in Figure 1C, the FWHM can also be found for each current response (labeled as τ_w). A larger FWHM means that the harvester can operate in lower frequencies and will result in a higher E_h. Finally, a characteristic single cycle for an open-circuit measurement is plotted in Figure 1D, where the y axis represents the change in open-circuit voltage. We define the open-circuit voltage response here not as the nominal open-circuit of the battery (around 3.7 V) but as the change in open-circuit voltage due to the application of stress. The voltage response is not symmetric with stress, so the entire peak-to-peak voltage difference is taken as the change in open-circuit voltage due to stress (ΔV_{OC}). To account for expected variations between pouch cells, we averaged ΔV_{OC} and ΔI_{SC} for at least three cells.

Now, we can quantify the performance of our pouch cell harvester using our derived figures of merit. For our system, $\Delta V_{OC} = 1.4 \pm 0.11$ mV and $\Delta I_{SC} = 2.53 \pm 0.077$ mA (plus or minus a standard deviation). Given an applied stress of $\Delta\sigma = 13$ MPa, the open-circuit voltage coupling factor is $K_{OC}(Li_yCoO_2, Li_xC_6) = 0.107\ \frac{mV}{MPa}$. The short-circuit current coupling factor for our cells is $G_{SC} = 1.85 \frac{\mu A}{cm^2 MPa}$ (for our cells, $A = 105\ cm^2$, which is the approximate area of the jelly-rolled cathode). Therefore, the normalized theoretical peak power density is $0.199\ \frac{nW}{cm^2 MPa^2}$. The FWHM of I_{SC} is $\tau_w = 300 \pm 20$ s, so our harvester has a normalized energy density of $59.6 \frac{nJ}{cm^2 MPa^2}$.

Comparing Low-Frequency Mechanical Harvesters Using Figures of Merit

With these figures of merit, we can now compare our system to a selection of other mechanical energy harvesters.[6,11–13,17,20–24] Table 1 presents only a subset of PEC harvesters[6,11–13,17] reported in the literature because not all mechano-electrochemical harvesters report the required data to calculate the figures of merit.[9,10,14,16,18] A

Table 1. Comparison of Selected PEC and Piezoelectric Harvesters Using PEC Figures of Merit

System[a]	f (Hz)	A (cm^2)	σ (MPa)	τ_w (s)	G_{SC} $\left(\frac{\mu A}{cm^2 MPa}\right)$	K_{OC} $\left(\frac{mV}{MPa}\right)$	Λ_{th} $\left(\frac{nW}{cm^2 MPa^2}\right)$	E_h $\left(\frac{nJ}{cm^2 MPa^2}\right)$
Li_yCoO_2 / Li_xC_6[b]	120e-6	105	13	300	1.85	0.107	0.199	59.6
Na_xBP[6]	0.005	2.25	0.2	100[c]	2.25	50.0	113	11,300
Li_xSi[11]	0.07	0.63	81[d]	3	0.179	0.278	0.0498	0.149
Li_xAl[12]	0.05	1	0.2	10[c]	4.00	45.0	180	1,800
Ionic diode[13]	0.014	4.52	0.25	5	2.72	28.0	76.2	381
Prussian blue[17]	0.05	4.5	530[d]	10[c]	0.0519	0.037	0.00192	0.0192
PMN-PT[20]	0.3	2.89	479	0.1[e]	0.0722	34.2	2.47	0.247
ZnO[21]	0.3	3	40	0.1[e]	4.17e-4	100	0.0417	0.00417
$BaTiO_3$[22]	2	1	1	0.1[e]	0.25	1.00e4	2,500	250
PVDF[23]	5	1.22	0.0052	0.1[e]	0.0158	3.84e4	549	54.9
PZT[24]	0.3	0.01	243	0.1[e]	0.494	39.2	19.4	1.94

The first six harvesters are PEC; the last five are piezoelectric.

[a]Not all PEC harvesters are compiled here; just the ones which reported ΔV_{OC}, ΔI_{SC}, and σ.

[b]Results from this paper.

[c]FWHM is defined as the total time stress was applied, but it might be higher if the device was operated at a slower frequency.

[d]Stress is hydrostatic stress, not uniaxial.

[e]For all piezoelectric systems, it is assumed $\tau_w = 0.1$.[11]

selection of piezoelectric harvesters that can operate under 10 Hz are also compared.[20–24] For papers that reported multiple device performances, the device in which the applied stress could be calculated was chosen. The detailed calculations for each system and all assumptions made are reported in the Supplemental Information (see Note S1).

In addition to the figures of merit, other important parameters are included in Table 1, such as active area A and applied stress σ. Also reported is the harvesting frequency f, which is calculated as the inverse of the total cycle time, which gives an idea of how low a frequency is at which this harvester is known to operate. However, this frequency might not be the lowest frequency possible for operation, so to get an idea for how low frequency the harvester can be, the FWHM of the short-circuit current is also reported (τ_w). Figures of merit G_{SC}, K_{OC}, Λ_{th}, and E_h reported in Table 1 are normalized to a single harvester. Because PEC harvesters must have two electrodes to work for ion movement, but piezoelectric harvesters typically only have one, the voltage outputs of the piezoelectric harvesters were scaled by a factor of 2 for a fair comparison.

As seen in Table 1, PEC systems, due to their higher FWHM values, can operate at much lower frequencies than piezoelectrics. Piezoelectric systems typically have higher K_{OC} and lower G_{SC} than PEC systems, indicating that PEC systems can outperform piezoelectric systems in normalized current density but need to be further optimized before they can compete with normalized voltage outputs. Since the stress needed to operate PEC systems is usually lower, normalized peak power density for PEC systems can be competitive with some piezoelectric systems, even though the actual peak power densities are much lower. Normalized half-cycle energy density, as expected due to higher theoretical energy densities, is typically higher for PEC systems than for piezoelectric systems. These results further highlight that PEC systems can fill a niche of low-frequency, high-energy-dense mechanical harvesters.

Our system has the highest reported FWHM and lowest harvesting frequency, but it does not perform as well in terms of energy density compared to other PEC harvesters. This is not surprising because LCO and graphite pouch cells are optimized for use as a battery, not for use as a mechanical harvester. A pouch cell is a well-studied, quality-assured system that produces a measurable PEC effect reliably and reproducibly, and as such is a good model system for this study. Nonetheless, the cells have a particularly low K_{OC}, which is as expected because the voltage coupling factor should correlate to the amount of expansion of the electrode during an electrochemical reaction,[5,7,15] and graphite and LCO have relatively low expansions,[5,25] which is more favorable for battery operation. Additionally, it is likely that the polymeric components in the pouch cell dissipate most of the mechanical energy[7,8] so the effective stress felt on the active materials might be much lower.

Comparing PEC harvesters, we can see that the decay rate of the short-circuit current (represented by the inverse of FWHM here) makes a major difference in the resulting energy density. This supports the claim that PEC harvesters need to maximize both coupling factors and minimize the decay rate.[5,15] However, there are not enough existing mechano-electrochemical harvesters to use these metrics to suggest new and better materials for researchers to try. We hope that as more researchers use these figures of merit to characterize their new harvesters, the field can gain insight into how to design and optimize better PEC energy harvesters.

Measuring the IV Curve for LCO and Graphite Pouch Cells

While these metrics use commonly reported information to compare mechanical harvesters' performance, they do not fully characterize the actual performance of the device under actual energy harvesting. To transfer power, harvesters will not operate at a open-circuit voltage (where there is no current flow) or short-circuit current (where voltage is zero) and instead will need to transfer charge across some finite impedance. Commercially viable harvesters might try to maximize power transfer by using impedance matching, which minimizes signal reflection from the load. Other applications might have external loads that are higher or lower impedances than the device impedance or even have impedances that change with time. A PEC harvester will not perform the same for different impedances, so it is important to understand how the system outputs will vary given any external load. To characterize the performance of our system under realistic operating conditions, we can look at another photovoltaic figure of merit called the fill factor (*FF*), which describes how the current and voltage outputs of the cell change with resistive loads.

FF is defined as the ratio of max power output to max theoretical power output (short-circuit current multiplied by open-circuit voltage). To calculate *FF*, photovoltaic systems measure an IV curve, which describes the change in current output with applied voltage bias. Graphically speaking, the *FF* is a measure of how square the IV curve of the system is (ideally, the system can maintain the short-circuit current at any applied voltage less than V_{OC}). Any deviation from a square indicates that, at that resistive load, the harvester's performance will be less than ideal; thus *FF* is a measure of the quality of the harvester. The max power output reported for PEC systems is usually theoretical max power, and not actual max power, which does not give any information on how the system will perform under realistic loads. Here, we measure a *FF* for our PEC harvester.

Mechanical energy harvesters must measure discrete points along an IV curve, instead of continuously changing the voltage bias, because the voltage and current outputs change with time. By using different-valued resistors (or applying different

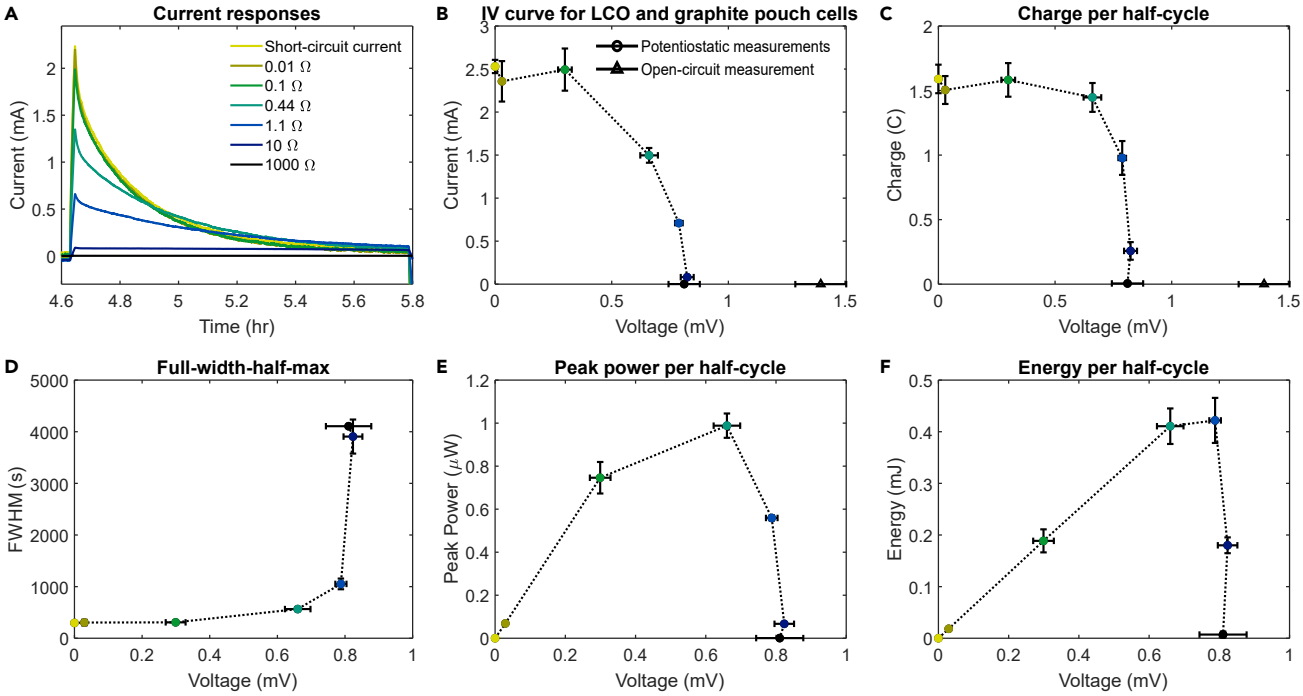

Figure 2. Measurement of an IV Curve for PEC Harvesters

(A) Current responses from representative half-cycles for each resistor.

(B) IV curve, with voltages calculated from Ohm's law. Colors on the potentiostatic measurements correspond to the resistors in 2A. Open-circuit voltage is marked as a triangle. Error bars mark plus or minus a standard deviation.

(C) The average charge per half-cycle, with corresponding resistor colors and standard deviation error bars.

(D) Average FWHMs at each resistance, with standard deviation. Open-circuit voltage is not included because it did not appreciably decay.

(E) Average peak power, with standard deviation.

(F) Average energy per half-cycle, with standard deviation.

current densities), which is analogous to putting a variable load on our harvester, we can approximate an IV curve. We soldered the positive terminal of our pouch cells to a resistor R with a value of 0.01, 0.1, 0.44, 1.1, 10, or 1,000 Ω. Using the same stress profile plotted in Figure 1B, we compressed the cells and the current response of the cells I_R was measured potentiostatically. The peak current for each resistor ΔI_R was defined similarly to ΔI_{SC} as the half peak-to-peak current.

A typical half-cycle current response with different resistors is plotted in Figure 2A (see Figure S2 for the full current response). As expected, different resistors yield different ΔI_R values and different decay rates. From the peak current outputs ΔI_R the corresponding voltage output was calculated from Ohm's law ($\Delta V_R = \Delta I_R R$). The resulting IV curve is shown in Figure 2B (each point's color corresponds to the color of the resistor labeled in Figure 2A). The error bars represent plus or minus the standard deviation of multiple cycles and multiple cells to account for the expected variation between pouch cells. Open-circuit voltage ΔV_{OC} is the only point on this curve that was measured in open-circuit mode, so it is marked separately in Figure 2B. The discrepancy between ΔV_{OC} and the voltage outputs for the larger resistors is due to an effect of frequency. To understand why $\Delta V_{1,000\Omega}$ is lower than ΔV_{OC}, we need to look at the charge of each half-cycle (calculated as the numerical integral of the current overtime) plotted in Figure 2C. It has been shown that the extracted charge from each cell should be the same, regardless of the resistor.[8] This is only true if we allow infinite time. From Figure 2C, we can see that the extracted

charge of the higher-valued resistors is much less than the extracted charge from the lower resistors, and this is likely responsible for the lower current outputs for these resistors. The full effect of frequency, however, requires further study.

To estimate the decay rate, the FWHM of each resistance is plotted in Figure 2D. The higher resistances (10 and 1,000 Ω) decayed too slowly for the half max to be reached; so FWHM for these resistances was just defined as the half-cycle time, even though it would likely be much higher. The lower resistors are able to decay sufficiently within the 120 μHz frequency. Finally, the peak power output of a half-cycle (calculated as $P_R = \Delta I_R^2 R$) and the total energy per half-cycle (calculated as the numerical integral of power over time) is plotted in Figures 2E and 2F (open-circuit voltage is excluded because the power and energy are zero). See Figure S5 for peak power plotted against a load (as is customary for piezoelectric harvesters).

The max peak power, from Figure 2E, is 0.99 μW, so using $\Delta I_{SC} = 2.53$ mA and $\Delta V_{OC} = 1.4$ mV, we calculate that the *FF* for these cells is 28%. This *FF* is significantly lower than most commercial silicon photovoltaic systems (which usually have at least a *FF* of 80%[26]). While the theoretical limit of *FF* for silicon photovoltaics is known,[26] the limit for PEC systems is not known, meaning we cannot determine whether a *FF* of 28% indicates a harvester approaching the limits of quality or one that requires more optimization. So *FF* can be used as a comparison of the relative quality between different PEC systems. It is still important to quantify because it will indicate how the system will perform under different loads.

While ideal power output is important for photovoltaic systems and piezoelectric systems, which have high power densities, PEC systems will primarily operate in energy density applications, so we also need to look at the energy performance of the system under realistic operating conditions. We can define an energy conversion efficiency (η_{EC}) that is analogous to the power conversion efficiency of photovoltaic systems and is the ratio of max energy per cycle to the input net mechanical energy per cycle. Note that this efficiency is distinct from the idealized bending energy efficiency that some harvesters report.[6,11] This idealized bending efficiency compares the ratio of the hydrostatic strain to the total strain energy as a function of Poisson's ratio. However, the efficiency we are proposing actually compares the input mechanical energy to the output electrochemical energy, as this is the more relevant conversion efficiency for the system[9] and is analogous to the k^2 metric used for piezoelectric harvesters.[27] This efficiency reveals the practicality of the system: how much energy one can get out for a given input energy.

For our pouch cells, the max energy per cycle is 0.844 mJ (twice the max energy per half-cycle in Figure 2F). We measure that the net mechanical work done by the Instron onto the pouch cell is 0.85 J for a full cycle (see Note S5 and Figure S4). Therefore, our energy conversion efficiency is 0.1%. Expected values for similar pouch cell systems range from 0.01 to 0.2 %.[5,8] For a similar LCO/graphite system at a faster frequency, the conversion efficiency was 0.01 %,[8] which suggests that frequency has a significant impact on the efficiency of the system. While these efficiencies are very low, it is important to keep in mind that a pouch cell is not an optimized system, as discussed earlier, and most of the input mechanical energy is likely dissipated in the non-active components of the pouch cell. A more optimized system would be able to withstand higher stresses, have higher coupling factors, and have minimal non-active material. What efficiencies an ideal system could reach is unknown—a thermodynamic limit for this process has not yet been derived. Due to the high possible efficiencies of Faradaic processes, the limit is expected to be

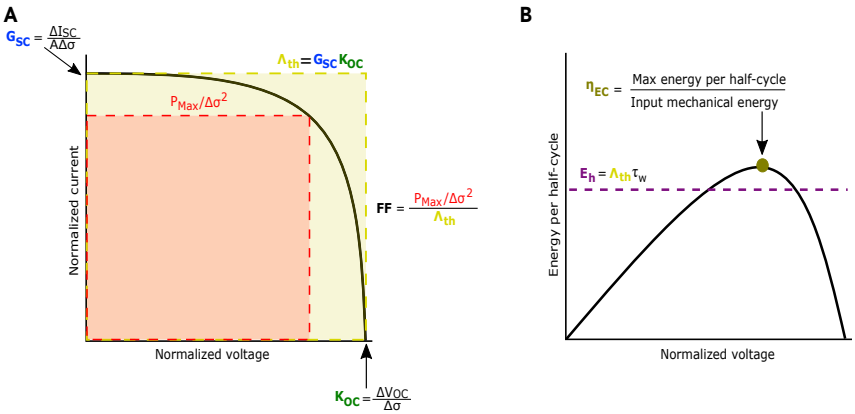

Figure 3. Summary of Mechano-Electrochemical Harvester Figures of Merit

(A) Schematic of an IV curve normalized by stress.

(B) Schematic of energy per half-cycle versus normalized voltage. Figures of merit are bolded.

orders of magnitude higher than what we achieve with a pouch cell. Regardless, the relatively low efficiency of these pouch cells indicates that there is the opportunity for significant optimization of these systems.

A summary of all proposed figures of merit is shown in Figure 3. As can be seen in Figure 3A, Λ_{th} is the upper limit to the possible max peak power (P_{max}). Though Λ_{th} is a still good approximation to compare different harvesters, *FF* is very important because it reveals how close the system is to ideal power production. Similarly, in Figure 3B, E_h can estimate the maximum energy per half-cycle (note it is not necessarily an upper-bound because the decay rate might be slower than $1/\tau_w$). To really characterize the practicality of the harvester, conversion efficiency η_{EC} is needed to tell how close the harvester is to ideal energy production.

A system could have high normalized current and voltage outputs and still not be commercially viable if its performance changes drastically with impedance. Both η_{EC} and *FF* are very low for our system, which is further confirmation of the conclusions from Table 1 that a pouch cell is not the best PEC energy harvester. Regardless, we can still use these pouch cell systems to study the PEC effect because they are convenient, have factory-level quality, and are easily combined into multiple configurations. As we show below, one can combine multiple pouch cells together to obtain higher device-wide current and voltage outputs than the fundamental material properties recorded in Table 1, which are normalized to a single harvester.

Combining PEC Harvesters in Series and Parallel Increases Voltage and Current

It has been speculated that the voltage output of mechano-electrochemical harvesters should add in a series configuration,[12] much like the voltages of serial-connected cells do (which has also been demonstrated in some piezoelectric devices[24]). Similarly, the current output of the harvesters should add in parallel. This has not yet been shown experimentally in PEC systems, so here, we demonstrate the effects of serial and parallel connections on ΔI_{SC} and ΔV_{OC} with our pouch cells. Note that it is vital to choose reference cells with a large enough capacity so that the current output of these harvesters is not limited. The parallel- and series-connected cells were two cells with the appropriate terminals shorted against one

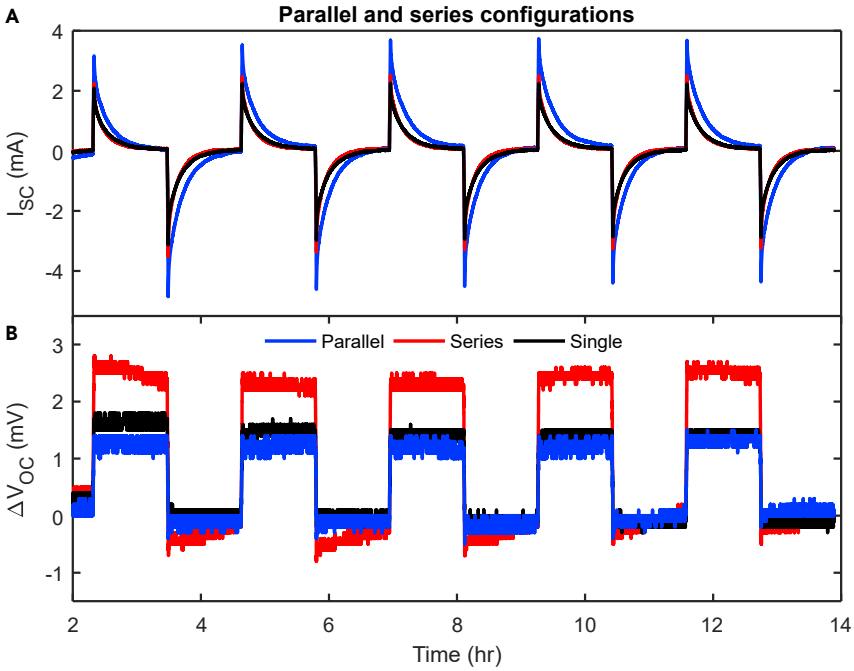

Figure 4. Short-Circuit Current and Open-Circuit Voltage Boosts with Series and Parallel
(A) Comparison of short-circuit currents using the potentiostat as an infinite reservoir. Short-circuit current ΔI_{SC} is higher in parallel cells.
(B) Comparison of the change in open-circuit voltages with respect to the initial V_{OC}. Open-circuit voltage increase ΔV_{OC} is higher in series cells.

another, with the potentiostat acting as an infinite capacity reservoir (in place of reference cells) to maximize current output.

Figure 4A plots five characteristic cycles of short-circuit current of a single cell compared to two cells connected in series or parallel (the first cycle is excluded because it is a formation cycle). Note that the coupling factors G_{SC} and K_{OC} are the same as in Table 1 because they are defined as coupling factors for a single system. However, the nominal current and voltage outputs are different in this setup. As expected, we see an improvement in ΔI_{SC} for the parallel setup over a single cell or series setup. Similarly, Figure 4B plots five characteristic cycles of the change in open-circuit voltage of the three configurations. Once again, as expected, we see the voltage increases with a series setup compared to a single cell or parallel setup. To quantify how much a series or parallel connection raises the outputs, Table 2 shows the average (with standard deviation) ΔI_{SC} and ΔV_{OC} for each configuration. The average FWHM for each is also tabulated (with standard deviation). Note that these standard deviations represent deviations within a single experiment, and not typical deviations between different pouch cells (see Figure S3).

With two cells in parallel, we get nearly double the ΔI_{SC} output compared to single or series configurations. Similarly, with two cells in series, we get double the ΔV_{OC} (within instrument error) compared to single or parallel. As seen in Table 1, PEC systems tend to have low K_{OC}, which limits their possible power densities. Table 2 indicates that PEC devices can overcome the problem of a low nominal voltage output if enough systems were connected in series. Also, cells connected in parallel have a larger FWHM (τ_w), which indicates that systems in parallel could harvest even lower frequency mechanical vibrations and reach even higher energy densities.

Table 2. Comparison of the Performance of a Single Working Cell to Two Working Cells Connected in Series or Parallel

Configuration	ΔI_{SC} (mA)	ΔV_{OC} (mV)	FWHM (s)
Single	2.58±0.028	1.48±0.057	290±31
Parallel	4.05±0.038	1.52±0.087	370±52
Series	2.89±0.018	2.94±0.17	240±31

Altogether, this proves promising because as higher K_{OC} and G_{SC} mechano-electrochemical systems are developed, serial and parallel connections will enable these devices to be viable for low-frequency mechanical-energy-harvesting applications.

Conclusions

Conventional mechanical energy harvesters such as piezoelectrics can provide low-energy sources to microelectronics by converting high-frequency mechanical vibrations to electrochemical energy at low-energy densities. Conversely, PEC energy harvesters can capture very low-frequency vibrations at high energy densities, but the current and voltage outputs are not yet comparable to other mechanical energy harvesters. To select and optimize mechano-electrochemical systems so that they become competitive with other mechanical harvesters, we need metrics to evaluate their applicability. Although photovoltaic figures of merit give us guidance on how to characterize PEC harvesters, we need to account for other experimental factors that affect PEC systems. To provide a methodology to consistently compare different mechano-electrochemical harvesters, we propose the following parameters: coupling factors G_{SC} and K_{OC}, and normalized power and energy densities (Λ_{th} and E_h),*FF* and energy conversion efficiency (η_{EC}). *FF* and efficiency are especially important parameters as they determine the efficacy of the PEC harvester under realistic operating conditions. We find that even our system, though not optimized, demonstrates the very low operating frequencies (τ_w = 300 s) and high energy densities (E_h = 59.6 $\frac{nJ}{cm^2 MPa^2}$) that make PEC systems desirable mechanical energy harvesters. We believe that more optimized PEC systems might be commercially viable for low-energy applications, especially if serial and parallel connections are used.

EXPERIMENTAL PROCEDURES

Resource Availability

Lead Contact

Further information and requests for resources should be directed to the Lead Contact, Craig B. Arnold (cbarnold@princeton.edu).

Materials Availability

This work did not generate new unique reagents.

Data and Code Availability

This work did not generate or analyze any datasets or codes.

Pouch Cell Preparation

Commercially available LCO and graphite 500-mAh pouch cells (GMB Power® 652535) were used for these experiments. It has been shown that there is an optimal SOC for energy harvesting[7,9] due to the highly nonlinear rate of expansion of the electrodes during lithiation.[25,28–30] To select the SOC for the pouch cells, we followed the procedure outlined in previous work[15,19] by measuring the differential expansion and differential voltage of the pouch cells (see Figure S1). The highest harvested energy corresponds to a high differential expansion and low differential

voltage. The SOC of the cells was chosen to be 12.5%. Cells were initially charge-cycled twice, and then after a rest step of at least 12 h, fully discharged, and then charged at a constant current of 50 mA (C/10) for 4,500 s to reach the selected SOC. Then, after another rest step of 12 h to allow for charge equilibration, the resistor was soldered to the positive terminal of the cell. Electrochemical measurements were performed with a 1287a Solartron potentiostat. The current output of the cells under compression was measured potentiostatically. Additionally, short-circuit current and open-circuit voltage outputs were measured with no added resistor.

Applied Stress Profile

The pouch cells were mechanically compressed in cycles using a compressive testing machine (Instron® 5969). The maximum stress placed on the cells was 13 MPa, even though a higher stress would have yielded a higher voltage.[5,7] Limiting the stress prevents mechanical failure of the polymer separator due to shorting and battery capacity fade due to the reduced pore size of a compressed separator.[31,32] A mechanical loading frequency of 120 μHz was used, with a mechanical loading and unloading rate of 13 MPa/min. For each experiment, three to six cycles were applied to the pouch cell, and three different cells were measured at each resistance, to account for the expected variation between different pouch cells.

Parallel and Series Preparation

After charging, two working cells were connected in series or parallel, and the charge between the two was allowed to stabilize for at least 12 h. Then both cells were compressed in the Instron, and short-circuit current or open-circuit voltage was measured with the potentiostat.

SUPPLEMENTAL INFORMATION

Supplemental Information can be found online at https://doi.org/10.1016/j.joule.2020.07.019.

ACKNOWLEDGMENTS

We would like to thank Nakita Noel for valuable discussions regarding photovoltaic systems, and Xinyi Liu for assistance with the experimental setup. We acknowledge financial support from Princeton University.

AUTHOR CONTRIBUTIONS

J.I.P. performed the main experiments and analyzed the data. S.K. assisted with experimental design and data analysis. C.B.A. supervised and guided the project and is the lead contact. J.I.P. was the primary author of the manuscript, which was reviewed and edited by S.K. and C.B.A.

DECLARATION OF INTERESTS

One of the authors is among the inventors of the patent US10680293B2.

Received: March 12, 2020
Revised: April 6, 2020
Accepted: July 21, 2020
Published: August 14, 2020

REFERENCES

1. Pu, X., Hu, W., and Wang, Z.L. (2017). Toward wearable self-charging power systems: the integration of energy-harvesting and storage devices. Small *14*, 1702817.
2. Cook-Chennault, K.A., Thambi, N., and Sastry, A.M. (2008). Powering MEMS portable devices – a review of non-regenerative and regenerative power supply systems with special emphasis on piezoelectric energy harvesting systems. Smart Mater. Struct. *17*, 043001.
3. Kim, H.S., Kim, J.H., and Kim, J. (2011). A review of piezoelectric energy harvesting based on vibration. Int. J. Precis. Eng. Manuf. *12*, 1129–1141.
4. Li, H., Tian, C., and Deng, Z.D. (2014). Energy harvesting from low frequency applications using piezoelectric materials. Appl. Phys. Rev. *1*, 041301.
5. Cannarella, J., and Arnold, C.B. (2015). Toward low-frequency mechanical energy harvesting using energy- dense Piezoelectrochemical materials. Adv. Mater. *27*, 7440–7444.
6. Muralidharan, N., Li, M., Carter, R.E., Galioto, N., and Pint, C.L. (2017). Ultralow frequency electrochemical–mechanical strain energy harvester using 2D black phosphorus nanosheets. J. ACS Energy Lett. *2*, 1797–1803.
7. Cannarella, J., Leng, C.Z., and Arnold, C.B. (2014). On the coupling between stress and voltage in lithium ion pouch cells. SPIE Sensing Technology + Applications *9115*, 91150K.
8. Schiffer, Z.J., and Arnold, C.B. (2018). Characterization and model of Piezoelectrochemical energy harvesting using lithium ion batteries. Exp. Mech. *58*, 605–611.
9. Jacques, E., Lindbergh, G., Zenkert, D., Leijonmarck, S., and Kjell, M.H. (2015). Piezo-electrochemical energy harvesting with lithium-intercalating carbon fibers. ACS Appl. Mater. Interfaces *7*, 13898–13904.
10. Sethuraman, V.A., Srinivasan, V., Bower, A.F., and Guduru, P.R. (2010). In situ measurements of stress-potential coupling in lithiated silicon. J. Electrochem. Soc. *157*, A1253–A1261.
11. Kim, S., Choi, S.J., Zhao, K., Yang, H., Gobbi, G., Zhang, S., and Li, J. (2016). Electrochemically driven mechanical energy harvesting. J. Nat. Comm. *7*, 10146.
12. Muralidharan, N., Afolabi, J., Share, K., Li, M., and Pint, C.L. (2018). A fully transient mechanical energy harvester. Adv. Mater. Technol. *3*, 1800083.
13. Hou, Y., Zhou, Y., Yang, L., Li, Q., Zhang, Y., Zhu, L., Hickner, M.A., Zhang, Q., and Wang, Q. (2016). Flexible ionic diodes for low-frequency mechanical energy harvesting. J. Adv. Mater. *7*, 1601983.
14. Massey, C.G., McKnight, G., Barvosa-Carter, W., and Liu, P. (2005). Reversible work by electrochemical intercalation of graphitic materials. Invited SPIE *5759*, 322–330.
15. Kang, S., Preimesberger, J.I., and Arnold, C.B. (2019). Varying power generation in ultra low-frequency mechanical energy harvesting of Piezoelectrochemical materials. J. Electrochem. Soc. *166*, A1704–A1708.
16. Harnden, R., Peuvot, K., Zenkert, D., and Lindbergh, G. (2018). Multifunctional performance of sodiated carbon fibers. J. Electrochem. Soc. *165*, B616–B622.
17. Zohair, M., Moyer, K., Eaves-Rathert, J., Meng, C., Waugh, J., and Pint, C.L. (2020). Continuous energy-harvesting and motion sensing from flexible electrochemical nanogenerators: toward smart and multifunctional textiles. ACS Nano *14*, 2308–2315.
18. Barvosa-Carter, W., Massey, C.G., McKnight, G., and Liu, P. (2005). Solid-state actuation based on reversible Li electroplating. Proc. SPIE 5761, Smart Structures and Materials 2005. Active Materials: Behavior and Mechanics *5761*, 90–97.
19. Schiffer, Z.J., Cannarella, J., and Arnold, C.B. (2016). Strain derivatives for practical charge rate characterization of lithium ion electrodes. J. Electrochem. Soc. *163*, A427–A433.
20. Hwang, G.T., Park, H., Lee, J.H., Oh, S., Park, K.I., Byun, M., Park, H., Ahn, G., Jeong, C.K., et al. (2014). Self-powered cardiac pacemaker enabled by flexible single crystalline PMN-PT piezoelectric energy harvester. Adv. Mater. *26*, 4880–4887.
21. Hu, Y., Zhang, Y., Xu, C., Zhu, G., and Wang, Z.L. (2010). High-output nanogenerator by rational unipolar assembly of conical nanowires and its application for driving a small liquid crystal display. Nano Lett *10*, 5025–5031.
22. Lin, Z.H., Yang, Y., Wu, J.M., Liu, Y., Zhang, F., and Wang, Z.L. (2012). $BaTiO_3$ nanotubes-based flexible and transparent nanogenerators. J. Phys. Chem. Lett. *3*, 3599–3604.
23. Sinha, T.K., Ghosh, S.K., Maiti, R., Jana, S., Adhikari, B., Mandal, D., and Ray, S.K. (2016). Graphene-silver-induced self-polarized PVDF-based flexible plasmonic nanogenerator toward the realization for new class of self powered optical sensor 8. ACS Appl Mater Interfaces *8*, 14986–14993.
24. Park, K.I., Son, J.H., Hwang, G.T., Jeong, C.K., Ryu, J., Koo, M., Choi, I., Lee, S.H., Byun, M., Wang, Z.L., and Lee, K.J. (2014). Highly-efficient, flexible piezoelectric PZT thin film nanogenerator on plastic substrates. Adv. Mater. *26*, 2514–2520.
25. Bucci, G., Swamy, T., Bishop, S., Sheldon, B.W., Chiang, Y., and Carter, W.C. (2017). The effect of stress on battery-electrode capacity. J. Electrochem. Soc. *164*, A645–A654.
26. Wang, L.X., Zhou, Z.Q., Zhang, T.N., Chen, X., and Lu, M. (2016). High Fill Factors of Si Solar Cells Achieved by Using an Inverse Connection Between MOS and PN Junctions. Nanoscale Res. Lett. *11*, 453.
27. Roscow, J.I., Pearce, H., Khanbareh, H., Kar-Narayan, S., and Bowen, C.R. (2019). Modified energy harvesting figures of merit for stress- and strain-driven piezoelectric systems. Eur. Phys. J. Spec. Top. *228*, 1537–1554.
28. Sethuraman, V.A., Van Winkle, N., Abraham, D.P., Bower, A.F., and Guduru, P.R. (2012). Real-time stress measurements in lithium-ion battery negative-electrodes. J. Power Sources *206*, 334–342.
29. Lee, J.H., Lee, H.M., and Ahn, S. (2003). Battery dimensional changes occurring during charge/discharge cycles—thin rectangular lithium ion and polymer cells. J. Power Sources *119–121*, 833–837.
30. Oh, K., Siegel, J.B., Secondo, L., Kim, S.U., Samad, N.A., Qin, J., Anderson, D., Garikipati, K., Knobloch, A., Epureanu, B.I., et al. (2014). Rate dependence of swelling in lithium-ion cells. J. Power Sources *267*, 197–202.
31. Cannarella, J., and Arnold, C.B. (2014). Stress evolution and capacity fade in constrained lithium-ion pouch cells. J. Power Sources *245*, 745–751.
32. Peabody, C., and Arnold, C.B. (2011). The role of mechanically induced separator creep in lithium-ion battery capacity fade. J. Power Sources *196*, 8147–8153.